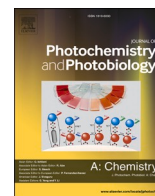




Contents lists available at ScienceDirect

Journal of Photochemistry & Photobiology, A: Chemistry

journal homepage: www.elsevier.com/locate/jphotochem

Binding of metal ions to the curcumin mediated methoxy polyethylene glycol thiol conjugated greenly synthesized gold nanoparticles: A fluorescence spectroscopic study

Shehab Al Shehab, Digambara Patra *

Department of Chemistry, American University of Beirut, Beirut, Lebanon

ARTICLE INFO

Keywords:

Binding
Methoxy polyethylene glycol thiol
AuNPs
Curcumin
Metal ions
Estimation

ABSTRACT

Curcumin, a nontoxic molecule obtained from plant extract, was used to reduce gold salt to produce gold nanoparticles (AuNPs). First time the particles were functionalized with methoxy polyethylene glycol thiol (mPEGT), which acts as a stabilizing agent in such a manner that the methoxy group is pointed toward the aqueous solution to serve as anchor point to many metal ions. The greenly synthesized gold nanoparticles have a size between ~40 and ~83 nm. The prepared material was characterized in detail by SEM, XRD, TGA and FT-IR spectroscopy. These AuNPs were found to be fluorescence active similar to free curcumin suggesting that curcumin is conjugated at the surface of AuNPs. Exposure of the mPEGT functionalized AuNPs to different concentrations of metal cations in the range between 0 and 100 μM resulted in the decrease in the fluorescence intensity of the AuNPs unlike free curcumin in aqueous solution. Excited state lifetime measurements further validated quenching mechanism to be static in nature. The binding constant and number of binding sites for such interaction were evaluated. Based on observed bimolecular quenching rate constants, k_Q values, the order of association of the metals studied is $\text{Pb (II)} > \text{Hg (II)} > \text{Hg (I)} > \text{Cd (II)} > \text{Al (III)} > \text{Ni (II)} > \text{Cu (II)} > \text{Na}_2\text{HAsO}_4$. These interactions between the mPEGT conjugated AuNPs and the metal ions in solution contribute a proof-of-concept that mPEGT functionalized curcumin mediated AuNPs can be used as a simple, cheap and straightforward, on-site detection system for toxic and even essential metal ions in solution.

1. Introduction

Designing and fabricating new fluorescence sensing systems for metal ions are of great demand because of their potential applications to chemo-sensors, a device that senses analyte with fluorescence signal transduction [1]. Fluorescent chemosensors are made up from a signaling unit or fluorophore and a guest-binding site or a receptor: the fluorophore and the receptor are usually separated by a spacer unit. Fluorescence is considered as the emission of photon after relaxation from an electronic excited state to the ground state [2]. Chemo-sensors based on changing in the fluorescence intensity are gaining great attention due to their simplicity of measurement, high efficiency and high sensitivity. The readout of a fluorescent chemosensor is usually a change in the fluorescence intensity, decay in lifetime or a shift in the emission wavelength [3].

Recently, several fluorescence spectroscopic approaches used quenching with metal ions as an approach to design highly sensitive

chemosensors. Captopril was studied for binding interaction with biologically active metal ions such as Mg (II), Ca (II), Mn (II), Co (II), Ni (II), Cu (II) and Zn (II) in an aqueous acidic medium by fluorescence spectroscopy [4]. A synthesized chemosensor was found to bind four different transition metal ions such as Hg (II), Cu (II), Ag (I) and Ni (II) in mixed aqueous solution at pH 7.2 [5]. Suwannee River fulvic acid was investigated for binding with several metal ions, only Al (III), Cu (II), Pd (II) and Tb (III) showed quenching of the fluorescence intensity [6]. Levofloxacin was studied for binding interactions with toxic metal ions such as Cd (II), Hg (II) and Pb (II) by fluorescence spectrophotometry. The metal ions quench the fluorescence intensity of LF by forming LF2-metal complex [7]. Moreover, silica nanoparticles having covalently linked luminescent chemosensors were also used, in this case copper, cobalt and nickel ions cause a strong quenching of the fluorescence intensity [8]. Three different anthrylaza crown ethers showed a decrease in fluorescence intensity upon binding of paramagnetic metal cations, like Mn (II)(d5), Co (II)(d7), Cu (II)(d9) [9]. Fluorescence

* Corresponding author.

E-mail address: dp03@aub.edu.lb (D. Patra).<https://doi.org/10.1016/j.jphotochem.2020.113083>

Received 23 October 2020; Received in revised form 26 November 2020; Accepted 2 December 2020

Available online 4 December 2020

1010-6030/© 2020 Elsevier B.V. All rights reserved.

lifetime quenching of molecular dyes near $d = 1.5$ nm of the AuNPs showed energy transfer to the metal surface [10]. Fluorophore-labeled DNA oligonucleotides showed extensive quenching when using divalent transition metal ions because of direct DNA-metal ion interactions, leading to combined static and dynamic quenching, with quenching rate increasing with the number of unpaired electrons in the metal ion and decreasing with the concentration of monovalent ions [11]. Dye-labeled histidine-containing peptides showed quenching with Cu (II) and Ni (II). A strong reduction in steady-state fluorescence was obtained and it was to be unaccompanied by any noticeable changes in lifetime kinetics. This static nature of quenching is not consistent with the dynamic Förster resonance energy transfer (FRET) phenomenon, which was assumed to dominate the quenching mechanism, and is likely caused by shorter range orbital coupling [12].

Heavy metal ions have originally become a world concern, because of their adverse health effects on human; these metal ions are detected in water and soil sources; making water and soil full of contamination [13]. For instance, lead toxicity has severe effects, such as renal malfunction and the brain development inhibition, so the serum level of lead in young children should not exceed 100 ppb [14]. Cadmium is well recognized for its negative influence on the enzymatic systems of cells, oxidative stress and for inducing nutritional deficiency in plants [15]. Furthermore, mercury can target the brain, as it remains the target organ for mercury, yet it can impair any organ and lead to malfunctioning of nerves, kidneys, and muscles. Also, it can cause disruption to the membrane potential and interrupt with intracellular calcium homeostasis. Mercury binds to freely available thiols as the stability constants are high [16]. The toxicity of heavy metal ions is well known, yet even essential metals such as zinc and copper are toxic at higher concentrations. In the past decade, several methods were used for the detection of metal ions; for example, atomic absorption spectroscopy [17], inductively coupled plasma mass spectrometry [18], electrochemical sensors [19] etc. However, these methods are expensive, time consuming, require sophisticated instruments, and trained staff. Therefore, a rapid, simple and cheap method for the determination of metal ions is of great desire for the public.

Metal nanoparticles, because of their unique optical, electronic, photonic, catalytic, and thermal properties, were widely researched in the past decade. AuNPs of size 3–100 nm are of high interest for detection of analytes, because their surface can be tuned by chemical modifications [20]. Due to the wide applications that AuNPs has, scientists around the globe are becoming more interested in environmentally friendly procedures for the synthesis of AuNPs by engineering processes to eliminate the use of hazardous substances through green chemistry. The usage of naturally occurring functionally rich biomaterials such as plant extracts or biomass can be an alternative to physical and chemical methods for the production of nanoparticles in an eco-friendly manner. Curcumin has a long history of use in food as a spice, mainly as an ingredient in many varieties of curry powders and sauces, wherein curcumin is the main coloring substance [21]. Recently, curcumin nano capsules were investigated as a potential photodynamic and anti-cancer activity enhancement [22]. Using plant extract such as curcumin exhibits the ability of reducing the nanoparticle through the hydroxyl and the carboxylic groups which play an important role in the reduction process of Au^{3+} to Au^0 [23]. Compared to chemical, physical and biological synthesis method, the green synthesis method is considered easy, environmentally friendly, and of lower cost [24]. Lately, highly orange red-emission gold nanoclusters synthesized by Curcuma longa root extract (CE) and 11- mercapto undecanoic acid (11-MUA) (CE/11-MUA-AuNCs) were used for the monitoring of three metal ions: Cd (II), Zn (II) and Cu (II). Fluorescence enhancement mechanism was observed for Cd (II) and Zn (II) ions, whereas fluorescence “turn-off” mechanism was observed for Cu (II) ion [25].

AuNPs were intensively employed in a variety of colorimetric detection of heavy metal ions [26]. Gold nanoparticles have strong absorption of electromagnetic waves in the visible region of the spectrum

due to the surface plasmon resonance (SPR), they can be synthesized easily and in straight forward manner, the gold core is chemically inert and nontoxic, they can be made highly stable with reduced dispersity and controlled size and shape, they have high surface-to-volume ratio, they can be functionalized by thiol linkage which can create gold nanoparticles for variety of applications, they are biocompatible because they can easily bind to biosystems such as bacteria, cells and proteins [27,28]. If there is a slight change in the nanoparticle like the size, shape, surface nature, or distance between particles, this can change their optical properties. Among the noble metal nanoparticles, gold nanoparticles are probably very studied, due to the relatively easy synthesis methods and to their inherent chemical and optical properties. Therefore, these particles can be used in applications such as design of optical devices, colorimetric sensors, surface-enhanced Raman scattering, localized surface plasmon sensing, bioimaging, and fluorescence-enhanced sensors [29]. Detecting the shifts in surface Plasmon resonance peak, accompanied by change in color, is because of change in the dielectric constant around the nanoparticles because of adsorption of analyte molecules, or due to analyte-induced agglomeration or aggregation of the nanoparticles [30]. The surface Plasmon absorption of AuNPs is also affected by metal ion binding [31]. PEG is a coiled polymer of repeating ethylene ether units with dynamic conformations. The addition of PEG to the gold NP surface (PEGylation) can reduce challenges such as aggregation due to passivated surfaces [32]. Through mPEGT (methoxy polyethylene glycol thiol), a stable Au-S bond can be formed. This organic monolayer is obtained through a self-assembly process, which results in a high stable multivalent system. To the best of our knowledge, this is the first work that describes binding of AuNPs conjugated mPEGT with metal ions by fluorescence spectroscopy. In this work, green synthesized AuNPs are established using a simple one-pot methodology with curcumin, as a reducing and methoxy PEGT as capping/conjugating agent to trap metal ions. These AuNP colloidal solutions were used as fluorescence sensors of different metal ions in aqueous solution such as Cd (II), Al (III), Cu (II), Na_2HAsO_4 , Pb (II), Hg (I), Hg (II), & Ni (II) ions and their binding affinity was established.

2. Materials and method

2.1. Materials

Methoxy Polyethylene Glycol Thiol and Gold (III) chloride were purchased from Acros. Curcumin was collected from Sigma Aldrich. Metal salts of Cd (II), Al (III), Cu (II), Na_2HAsO_4 , Pb (II), Hg (I), Hg (II), Ni (II) were obtained from Sigma Aldrich. These chemicals were used without any further purification and dissolved in double distilled water. Curcumin was dissolved in methanol.

2.2. Synthesis of methoxy poly ethylene glycol thiol conjugated AuNPs using curcumin

In order to achieve mild basic conditions of pH 13, few pellets of NaOH were dissolved in double distilled water and 1 mL of it was added to the final mixture. Since curcumin is insoluble in water, methanol was used to dissolve it. 30 mM of mPEGT were dissolved in 15 mL of DDW (double distilled water) and kept at 45 °C for 15 min. Then, 1 mM of HAuCl_4 dissolved in 15 mL of DDW was added. Finally, curcumin of 10 mM and 1 mL solution (dissolved in methanol) was added to the solution. The entire solution was kept in the oven at 45 °C for 24 h. To separate the gold nanoparticles and the curcumin solution, the final solution was centrifuged at 15,000 rpm for 25 min at 20 °C, the upper phase which is constituted of undissolved curcumin was discarded and the lower phase of gold nanoparticles which has a clear intense purple color were kept and diluted to 15 mL.

2.3. Sample preparation for metal ion binding

For sensing/binding study of metal ion, 1 mM of metal ion was dissolved in 15 mL of DDW to prepare the stock solution. To prepare different concentrations of metal ions ranging between 0 and 100 μM , 200 μM of gold nanoparticles was added into labeled vials, then desired volume of metal ion was added to achieve the desired concentration, then the volume was completed to 3 mL. The study was established by fluorescence spectroscopic measurements with an excitation wavelength of 425 nm.

2.4. Instrumentation

The absorption spectra were recorded at room temperature using a JASCO V-570 UV-vis-NIR spectrophotometer. Scanning electron microscopy (SEM) analysis was done using Tescan, Vega 3 LMU with Oxford EDX detector (Inca XmaW20). The SEM pellet was prepared as follow, few drops of diluted gold solution were settled on an aluminum stub and coated with carbon conductive adhesive tape. FTIR spectra were recorded on a FTIR-Raman spectrometer. A Thermo Nicolet 4700 Fourier Transform Infrared Spectrometer equipped with a Class 1 laser was used for this purpose. The KBr pellet technique was applied to perform the transmission experiments in the range between 3200 and 700 cm^{-1} . The Thermogravimetric Analysis (TGA) measurements were done using a Netzsch TGA 209 in the temperature range 30–800 $^{\circ}\text{C}$ with an increment of 10 $^{\circ}\text{C}$ / min in a N_2 atmosphere. Fluorescence spectrum was measured using Jobin-Yvon-Horiba Fluorolog III fluorometer and the FluorEssence program. The excitation source was a 100 W Xenon lamp, and the detector used was R-928 operating at a voltage of 950 V instrument by keeping the excitation and emission slits width at 5 nm. The emission and excitation measurements were documented with resolution increment 1 nm and slit 5 nm using the same machine.

3. Results and discussion

3.1. Synthesis and characterization of curcumin mediated mPEGT AuNPs

3.1.1. Visual identification of AuNPs

A detailed study of synthesis of gold nanoparticles by mPEGT was carried out in this work. Figure S1 (see Supporting Information) shows the tautomerization reaction between curcumin enol and keto form, which was used as a reducing agent. Curcumin of bright yellow color is a diarylheptanoid. It is considered as a curcuminoid, which are considered natural phenols. This tautomer is present in its enolic form in organic solvents and in keto-enol form in water [24]. After adding curcumin to the Au salt HAuCl_4 , a yellow color was first observed, then after achieving mild basic conditions through NaOH, dark pink color appeared in the solution indicating the formation of the gold nanoparticles where the whole solution was incubated in the oven for 24 h to achieve an intense color. This color change indicates the formation of the gold nanoparticles. The origin of such coloration is caused by the interaction of the electromagnetic field with the collective oscillation of free conduction electrons; the resonances are named SPR (Surface Plasmon resonance) [33]. Then centrifugation was used to separate the gold nanoparticles and the undissolved curcumin solution, the upper phase which is constituted of undissolved curcumin was discarded and the lower phase of gold nanoparticles which has a clear intense purple color were kept and diluted to 15 mL.

3.1.2. UV-vis absorption spectroscopy and SEM studies

This formed colloidal solution obtained after centrifugation has a very intense dark purple color, which was inspected by UV-vis absorption spectroscopy, where the characteristic peak of AuNPs was obtained at wavelength of 539 nm (see Fig. 1A). The electronic spectra of curcumin dissolved in methanol is shown in Fig. 1B. Curcumin in methanolic solution showed a broad characteristic UV-vis absorption at

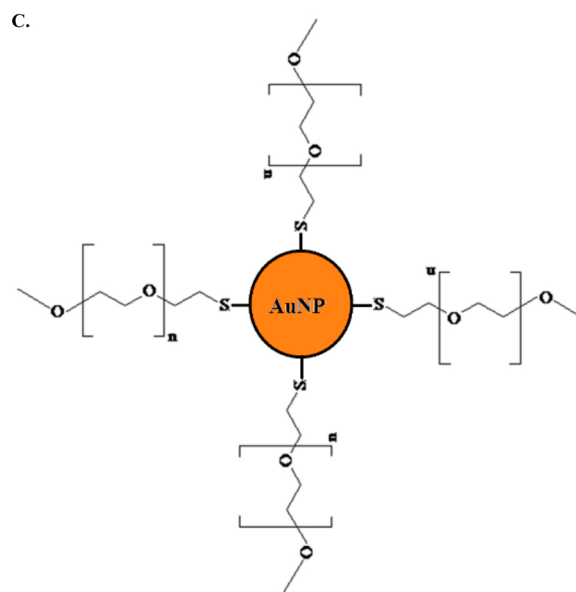
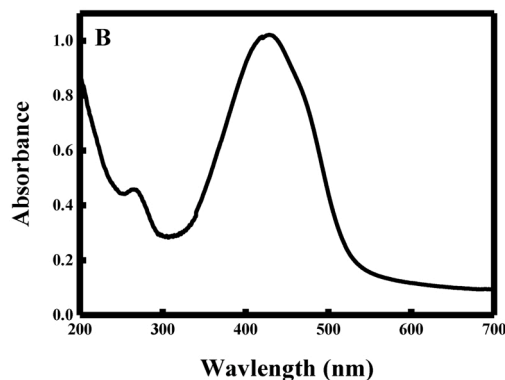
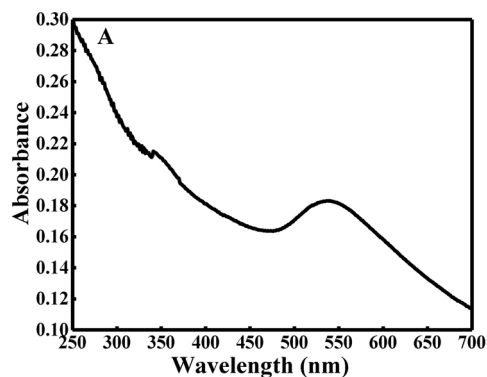


Fig. 1. (A) UV-vis absorption spectrum of PEG thiol conjugated AuNPs measured after 24 h; (B) UV-vis absorption spectrum of curcumin dissolved in methanol; (C) Illustration of ligands containing methoxy PEG-SH used to functionalize the surface of gold nanoparticle.

around 300–500 nm with maximum absorption band at wavelength 424 nm and a weak absorption band at 262 nm. The purple color of gold nanoparticles will be transformed to pink after dilution. mPEGT is chemically linked to the gold surface through Au-Sulfur bond. The other end constituting the methoxy group is pointing toward the colloidal suspension or solution as shown in Fig. 1C. From SEM image given in Fig. 2A, B and C, it can be deduced that the morphology is spherical for

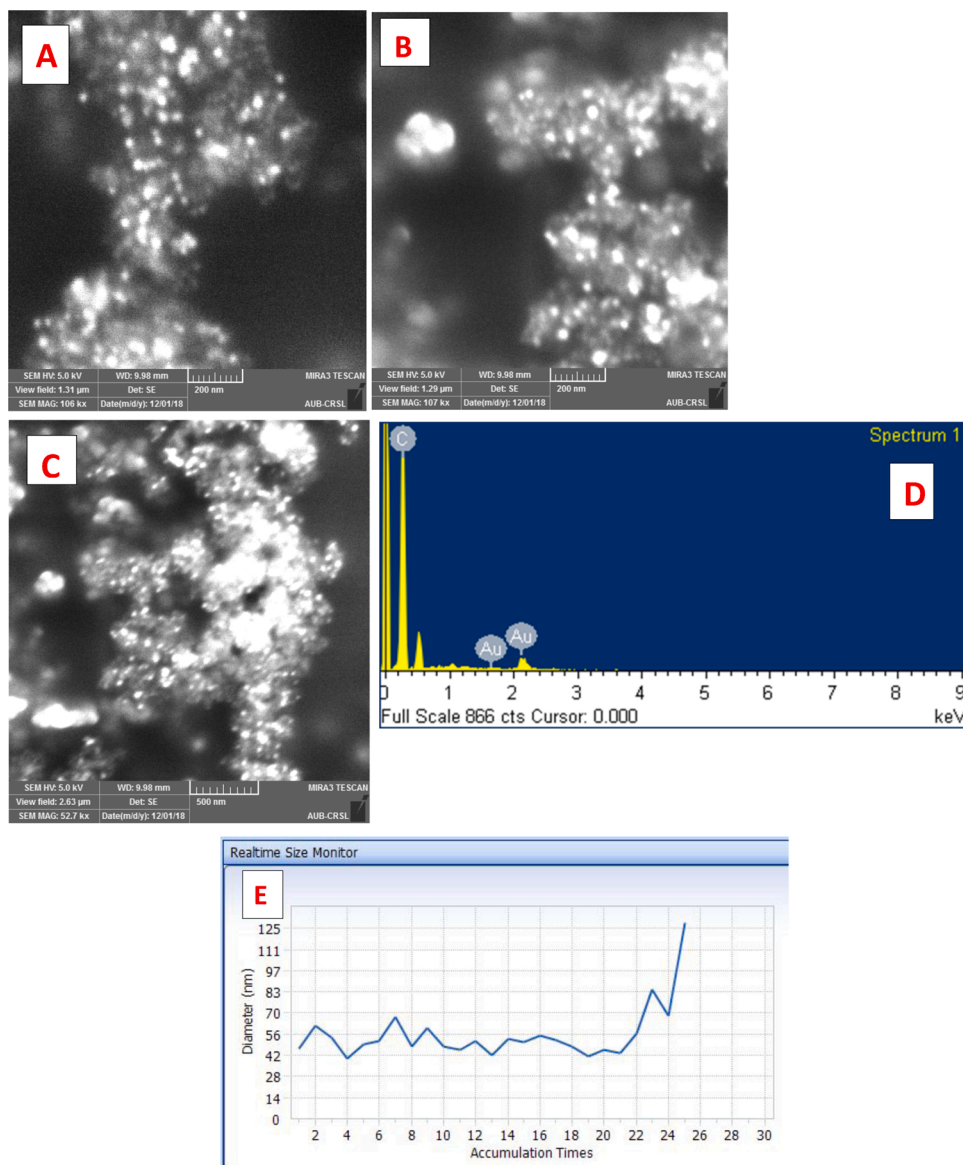


Fig. 2. (A) and (B) and (C) SEM images reveal that the mPEGT functionalized AuNPs retain their roughly spherical shape, and (D) corresponding EDX image and (E) Particle size distribution value of PEGylated AuNPs at pH 13.

the gold nanoparticles. Corresponding EDX analysis is provided in Fig. 2D confirming presence of Au and C (carbon) due to curcumin and mPEGT. From Fig. 2E, the particle size distribution (DLS) can be deduced, the particles have size ranging between 40 and 83 nm.

3.1.3. XRD, TGA and FTIR studies

A representation of the XRD pattern of mPEGT conjugated AuNPs is shown in Fig. 3. AuNPs showed characteristic peaks at 38.269° , 44.600° , 64.678° , and 77.549° . The Bragg reflections attributed to the (111), (200), (220), and (311) sets of lattice planes are seen that may be indexed on the basis of face centered cubic structure of Au [34]. The XRD pattern thus clearly shows that the Au nanoparticles formed by the reduction of AuCl_4^- ions by curcumin are crystalline in nature.

Fig. 4A shows FTIR spectrum of curcumin and AuNPs obtained by curcumin and mPEGT stabilizing agent. Curcumin showed a peak at 3508 cm^{-1} which corresponds to phenolic O—H stretching vibration, another peak was observed at 1628 cm^{-1} which is associated to the aromatic moiety C=C stretching, another peak at 1509 cm^{-1} corresponds to C=O and C=C vibrations, and 1428 cm^{-1} corresponds to olefin C—H bending vibrations [35]. For the AuNPs synthesized using

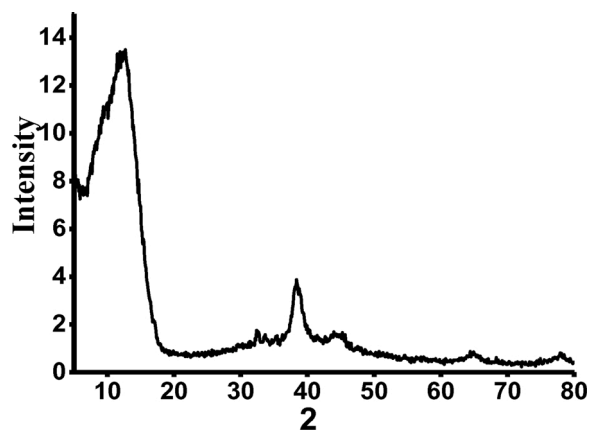


Fig. 3. XRD patterns observed for mPEGT conjugated Au nanoparticles.

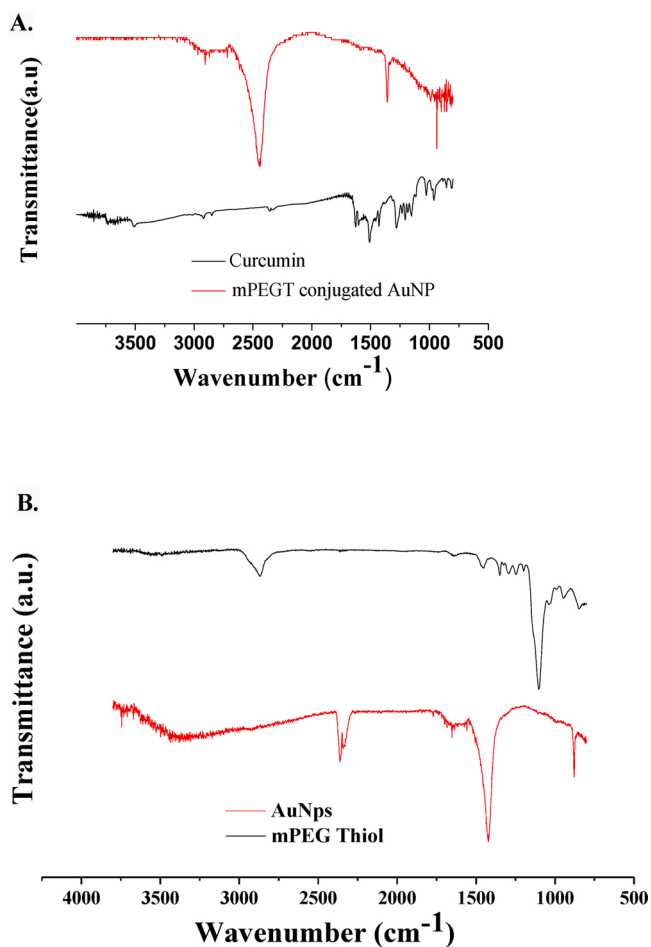


Fig. 4. (A) FTIR spectrum of curcumin shown in black and AuNPs in Red; (B) FTIR spectrum of the polymer mPEG thiol shown in black and AuNps shown in red.

mPEGT, a peak was observed at 668.28 cm^{-1} which corresponds to the C–S stretching, the peaks corresponding to the SH stretching appear in the region $2600\text{--}2540\text{ cm}^{-1}$ were also observed [36]. Fig. 4B shows the FTIR of mPEGT and AuNPs. The characteristic peaks for mPEGT are: 2868.34 cm^{-1} which corresponds to C–H stretching of alkane, 1103 cm^{-1} which corresponds to C–O stretching, and a peak of 639.5 cm^{-1} which corresponds to C–S stretching.

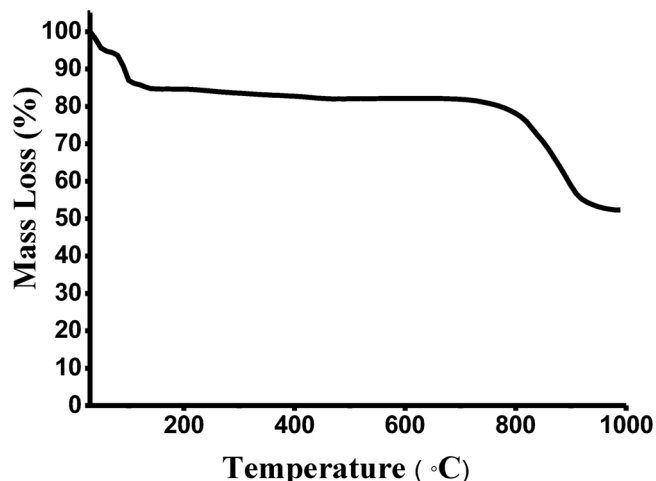


Fig. 5. TGA of mPEGT functionalized gold nanoparticles.

The AuNPs were converted to powder form before performing TGA analysis. Under inert N₂, TGA was performed heating the gold nanoparticle powder from 30 to 1000 °C which is presented in Fig. 5. 15 % weight loss was observed between 30–130 °C. This weight loss corresponds to water loss of our sample. Between 170–420 °C, organics is expected to degrade, so around 5 % of curcumin and mPEGT weight loss was obtained. Around 30 % of mPEGT is degraded at 700 °C this is because of the strong attachment of thiol bond of mPEGT to the gold surface [37].

3.2. Binding of AuNPs with metal ions

3.2.1. Fluorescence quenching study

The fluorescence spectrum of mPEGT conjugated AuNPs was measured at 425 excitation wavelength and scanned in the emission wavelength range between 440 and 700 nm as shown in Fig. 6A and B (the top black colored spectrum at 0 μM of metal ion). Two peaks were observed, one minor humps at ~496 nm due to Raman scattering (normally observed in aqueous media when fluorescence intensity is relatively weak [38]) and the other at ~540 nm due to fluorescence emission. This fluorescence spectrum is similar to the fluorescence of curcumin in the aqueous environment [38] indicating curcumin is conjugated along with mPEGT at the surface of AuNPs.

With the successful functionalization of stable mPEGT AuNPs, a series of di- and trivalent metal ions were titrated into a solution of mPEGT modified AuNPs in double distilled water. Various concentrations of each metal ion between 0 and 100 μM in DDW were pipetted into

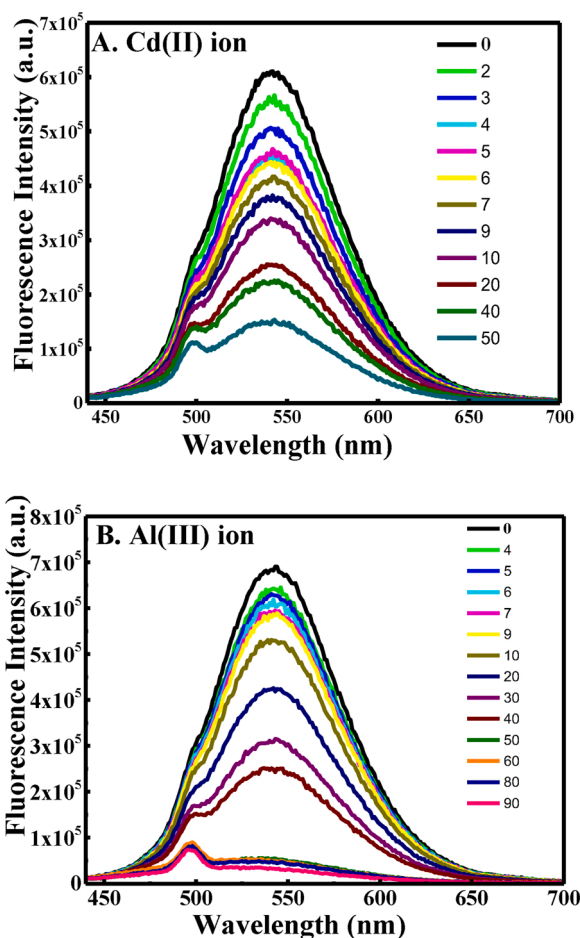


Fig. 6. Fluorescence emission spectra excited at $\lambda = 425\text{ nm}$ for mPEGT conjugated AuNPs titrated with varying concentrations of (A) Cd (II) and (B) Al (III) ions.

mPEGT AuNP solution. The solution was incubated at room temperature ($\sim 21^\circ\text{C}$) in order to allow for complexation between mPEGT and the divalent and trivalent metal cations. The tested metal ions were respectively Cd (II), Al (III), Cu (II), Na_2HAsO_4 , Pb (II), Hg (I), Hg (II) and Ni (II). Before running fluorescence spectral measurement, the solution was vortexed for 30 s to make sure of the homogeneity of the solution. Fig. 6 depicts fluorescence spectra of PEGT conjugated AuNPs for various concentrations of representative Cd (II) and Al (III) ions. The initial fluorescence intensity of the mPEGT functionalized gold nanoparticles which was monitored at 540 nm decreased regularly as the metal ion concentration was increased from 0 to 100 μM .

However, as seen in Fig. 6 the emission maximum of AuNPs did not change in the presence of metal ions which suggest that solvent environment around AuNPs remains the same. With further increase in metal ion concentrations, there was also no significant shift of $\lambda_{\text{em}}^{\text{max}}$, which suggests there was also no conformational change of the conjugating ligands around AuNPs under the condition studied here. Nevertheless, the intrinsic fluorescence quenching of mPEGT conjugated AuNPs in the presence of metal ions indicates complex formation between AuNPs and metal ions. The detailed fluorescence quenching mechanism was studied and will be discussed later on. Similar results were obtained for other metal ions under investigation.

Although unreacted and free curcumin was removed after centrifugation, curcumin attached with mPEGT conjugated AuNPs during preparation may directly bind with metal ions and influence the fluorescence properties of mPEGT conjugated AuNPs. To test this possibility, interaction of free curcumin in aqueous environment (in DDW as used for mPEG conjugated AuNPs) with various metal ions was investigated. It is reported in literature that fluorescence of curcumin is quenched by Hg (II) ions [39,40] whereas Ni (II), Cu (II) and other metal ions have no influence on fluorescence of free curcumin, interestingly in the present case it was found that presence of Hg (II) ions in solution in the concentration under studied enhanced the fluorescence intensity of free curcumin (see Figure S2A, Supporting Information). This contrast in the present results could be due to use of organic solvent/host molecule in the literature [39,40] which facilitate curcumin to come in close contact with Hg (II) ions. Similar results were found in the presence of Ni (II) (see Figure S2B, Supporting Information) and Hg (I) (not shown) ions. In the present case the enhancement could be due to aggregation/dimerization of hydrophobic curcumin in the presence of metal ions. Therefore, the observed fluorescence quenching of mPEGT conjugated AuNPs in the presence of metal ion is different from the interaction of free curcumin with metal ion. It is reported earlier that metal ions often binds with the methoxy group of the ligands [31]. Therefore, it can be speculated that the metal ions bind with the AuNPs through the methoxy group of the mPEGT associated with AuNPs.

Gold nanoparticles functionalized with polymers have been proven an efficient detection system [41]. Quenching of the adsorbed fluorophore is observed, and recovery is monitored after disruption of this adsorption by a target [41]. Because it is considered easy to functionalize gold nanoparticles, different recognition elements & chemical groups can be adsorbed in order to create chemical sensors. In our case methoxy group of mPEGT is pointing toward the solution as depicted in Fig. 1(C) and it can be deduced that methoxy ether groups adsorbed to the gold nanoparticles can bind both divalent and trivalent metal ions [31]. An interaction between two molecules usually causes changes in the fluorescence parameters such as quantum yield, intensity or lifetime. There are several types of mechanisms of quenching called collisional, static, electron transfer or energy transfer at a distance known also as Förster energy transfer. The difference between collisional and static is that in collisional, two molecules diffuse inside the solution and collide because of internal motion or local flexibility. This dynamic quenching occurs during the lifetime of the excited state. However, in static quenching, the quencher molecule binds to the target forming a complex. In this case, quenching takes place by forming a non-fluorescent complex at the ground state. When the complex absorbs light, it

directly returns to the fundamental state without emitting any photons [42]. In the case of collisional quenching, the quenching fluorescence intensity can be described by the Stern–Volmer equation:

$$\frac{I_0}{I} = 1 + K_{SV} [\text{metal ion}] = 1 + k_Q \tau_0 [\text{metal ion}]$$

Where I_0 and I are the fluorescence intensities in the absence and presence of metal ion respectively, K_{SV} is the Stern–Volmer constant, k_Q is the bimolecular quenching constant expressed in $\text{M}^{-1}\text{s}^{-1}$, τ_0 is the excited state lifetime of the AuNPs in the absence of metal ion and $[\text{metal ion}]$ is the metal ion concentration. This equation describes that the higher the K_{SV} , the lower concentration of metal ion needed to decrease fluorescence intensity. Plotting I_0/I as a function of $[\text{metal ion}]$ yields a linear plot (representative graphs shown in Fig. 7) with a slope equal to K_{SV} . Our results show that Hg (II) and Pb (II) are the two most ions that have the higher K_{SV} (see Table 1).

For the determination of k_Q , the excited state lifetime of mPEGT conjugated AuNPs was measured in the absence of metal ion using a 405 nm excitation laser and emission was collected at 540 nm. The fluorescence decay profile as shown in Figure S3 (see Supporting Information) could be best fitted with a biexponential decay. The excited state lifetimes were found to be 1.17 ns ($\sim 20\%$) and 4.84 ns ($\sim 80\%$) with an average lifetime of 4.22 ns. The minor first component of excited state lifetime value of mPEGT conjugated AuNPs is about 2-fold higher than that of the free curcumin reported in aqueous environment [33], however, the second component of excited state lifetime value of mPEGT conjugated AuNPs is within the error margin of free curcumin [33]. This implies that conjugation of curcumin at the surface of AuNPs does influence the excited state properties though it does not change the

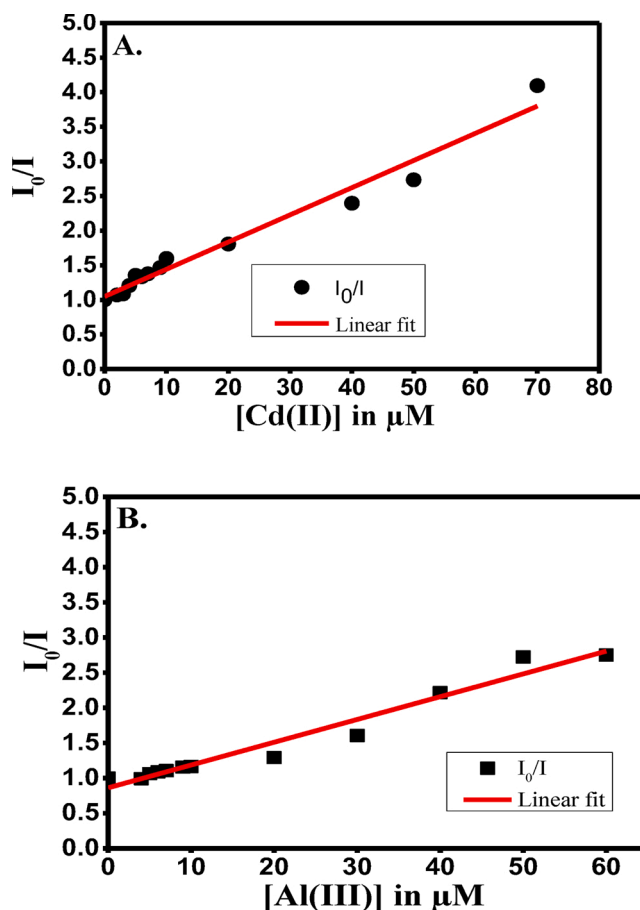


Fig. 7. Stern–Volmer plot for fluorescence quenching of mPEGT conjugated AuNPs by (A) Cd (II) ion and (B) Al (III) ion.

Table 1

Stern-Volmer constant (K_{sv}) and bimolecular quenching rate constant (k_Q) for the fluorescence quenching of mPEGT conjugated AuNPs by various metal ions.

Metal ion	$K_{sv}(M^{-1})$	$k_Q (M^{-1}s^{-1})$
Cd (II)	3.93×10^4	9.31×10^{12}
Al (III)	3.23×10^4	7.65×10^{12}
Cu (II)	2.86×10^4	6.78×10^{12}
Na_2HAsO_4	1.77×10^4	4.19×10^{12}
Pb (II)	3.46×10^5	8.20×10^{13}
Hg (I)	9.00×10^4	2.13×10^{12}
Hg (II)	1.01×10^5	2.39×10^{13}
Ni (II)	2.47×10^4	5.85×10^{12}

energy gap between HOMO and LUMO of free curcumin. The k_Q values for mPEGT conjugated AuNPs in the presence of different metal ions were estimated using average excited state lifetime of 4.22 ns and given Table 2. For dynamic quenching, the maximum value of k_Q is in the range of 1×10^{10} [43]. However, in this study, the obtained values are in the order of 10^{12} and 10^{13} . This quenching rate constant value suggest the quench reaction between mPEGT conjugated AuNPs and metal ions is diffusion-controlled reaction. This very large value of K_{sv} suggests that a static quenching sphere quenching mechanism is operative envisaging the presence of AuNPs and metal ions in close proximity within the quenching sphere of action [44]. This quenching sphere of action model assumes the existence of a sphere around the fluorescence molecule within which the probability of immediate quenching is unity. Such quenching process is extremely fast, in picosecond time scale, and effectively de-excites all the fluorescent molecules (AuNPs) without the involvement of the molecular diffusion. The only observable fluorescent molecules (AuNPs) are those for which there are no quencher in this sphere. This quenching mechanism was further established by measuring excited state lifetime in the presence of various concentration of metal ions such as Pb (II) and Ni (II) ions. It is found that the average excited state lifetime of mPEGT conjugated AuNPs in the presence of Pb (II) ion did not change remarkably, which was similar to most of the metal ions except of Ni (II) ions where a slight decrease (within 15 % even at the highest concentration of Ni (II) ions) in the excited state lifetime was observed as summarized in Table 2. Interestingly, when UV-vis absorption spectra were measured with increasing the concentration of the metal ions, no trend was observed for all metal ions except for Cadmium (see Figure S4, SI).

3.2.2. Binding constant and binding sites

In static quenching, there exist a relationship between intensity and the concentration of quencher which is represented below [45]. Binding of small molecules like metal ions with independently set of equivalent sites in a macromolecule like methoxy poly ethylene glycol layer around the gold nanoparticle can be expressed through the equilibrium between free and bound molecules as [45]

$$\log \frac{I_0 - I}{I} = \log K + n \log [\text{metal ion}]$$

Where K and n are the binding constant and the number of binding sites,

Table 2

Excited state lifetimes of mPEGT conjugated AuNPs in the presence of varying concentrations of Pb (II) and Ni (II) ions. The excited state lifetime was measured at $\lambda_{exc} = 405 \text{ nm}$ and $\lambda_{em} = 540 \text{ nm}$.

Metal ion	[Metal ion] in μM	τ_1 (ns)	Relative Amplitude (%)	τ_2 (ns)	Relative Amplitude (%)	τ_{average} (ns)	χ^2
Pb (II)	0	1.17	20.12	4.84	79.88	4.22	1.46842
	3.33	1.82	14.23	4.73	85.77	4.25	1.34674
	16.66	1.23	13.57	4.68	86.43	4.21	1.50051
	33.33	1.46	20.32	4.82	79.68	4.14	1.60473
	0	1.17	20.12	4.84	79.88	4.22	1.46842
Ni (II)	1.66	1.42	42.93	5.52	57.07	3.77	2.39604
	16.66	1.33	40.07	5.20	59.93	3.66	2.28959
	33.33	1.3	48.19	5.69	51.81	3.58	2.18988

respectively. This can be estimated by plotting $\log \{(I_0 - I)/I\}$ versus $\log [\text{metal ion}]$ (see Fig. 8 for representative graph of Hg (I) ion)). The best fits obtained provided n values that ranged from 0.42 for arsenic to 1.7 for Al (III) ion (see Table 3). The K values ranged from $3.43 \times 10^8 \mu\text{M}$ for Al (III) ion to $3.18 \times 10^1 \mu\text{M}$ for As ion. The number of the binding sites can provide insight about the number of sites in the gold nanoparticle that is associated with the metal ion. For instance, Cd (II), Cu (II), and Hg (II) almost bind the mPEGT mediated AuNPs at 1 site. On the other hand, two molecules of these ions (Arsenic, Hg (I) and Pb (II) ions) bind to one AuNPs. However, Al (III) almost bind two gold nanoparticles.

4. Conclusion

Evidently, methoxy poly ethylene glycol thiol was used to functionalize greenly synthesized gold nanoparticles, reduced by curcumin which is a nontoxic plant extract. The size of the gold nanoparticles was between 40 - 83 nm. The green synthesized gold nanoparticles were used to afford an analytical fluorescence method for the determination of metal binding of a number of metal ions in aqueous solution. The curcumin mediated mPEGT conjugated gold nanoparticles showed highest respective binding for Pb (II), Hg (II), Hg (I), Cd (II), Al (III), Ni (II), Cu (II) and As. Steady state fluorescence and excited state lifetime measurements established that a static quenching sphere mechanism is operative envisaging the presence of AuNPs and metal ions in close proximity within the quenching sphere of action. This fluorometric method provides a prototype for a new method to analyze metal cations in solution.

CRedit authorship contribution statement

Shehab Al Shehab: Methodology, Data curation, Investigation,

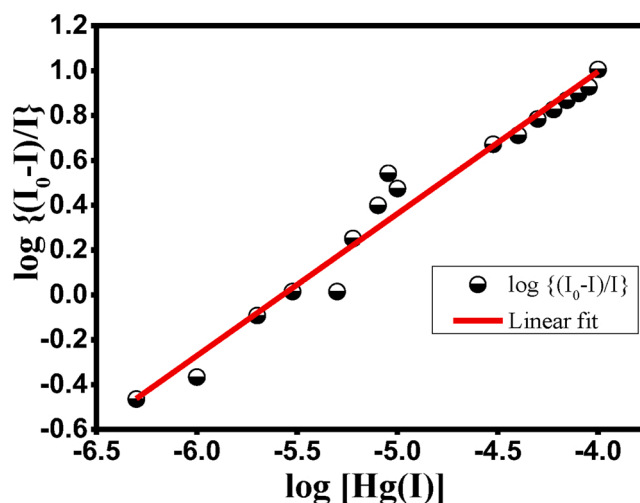


Fig. 8. Plot of $\log\{(I_0 - I)/I\}$ vs. $\log [\text{Hg (I)}]$ for the estimation of binding constant (K) and number of binding sites (n).

Table 3

Binding constant (K) and number of binding sites (n) of various metal ions while associating with mPEGT conjugated AuNPs.

Metal ion	n	K (M ⁻¹ s ⁻¹)
Cd (II)	0.96	2.96 × 10 ⁴
Al (III)	1.88	3.43 × 10 ⁸
Cu (II)	1.33	2.61 × 10 ⁶
NaHAsO ₄	0.42	3.18 × 10 ¹
Pb (II)	0.45	5.58 × 10 ²
Hg (I)	0.63	3.38 × 10 ³
Hg (II)	0.73	6.65 × 10 ³
Ni (II)	0.67	1.44 × 10 ³

Validation, Formal analysis, Writing - original draft. **Digambara Patra:** Conceptualization, Supervision, Resources, Project administration, Writing - review & editing.

Declaration of Competing Interest

The authors declare that they have no known competing financial interests or personal relationships that could have appeared to influence the work reported in this paper.

Acknowledgments

Financial support provided by American University of Beirut, Lebanon through URB as well as Kamal A. Shair Central Research Laboratory (KAS CRSL) facilities to carry out this work is greatly acknowledged.

Appendix A. Supplementary data

Supplementary material related to this article can be found, in the online version, at doi:<https://doi.org/10.1016/j.jphotochem.2020.113083>.

References

- [1] K. Yoshida, T. Mori, S. Watanabe, H. Kawai, T. Nagamura, Synthesis and metal ion-sensing properties of fluorescent PET chemosensors based on the 2-phenylimidazo [5,4-a]anthraquinone chromophore, *J. Chem. Soc. Perkin Trans. 2* (1999) 393, <https://doi.org/10.1039/a900424f>.
- [2] J.R. Lakowicz, *Principles of Fluorescence Spectroscopy*, Springer, New York, NY, 2013.
- [3] L. Fan, Y. Zhang, C. Murphy, S. Angell, M. Parker, B. Flynn, et al., Fluorescent conjugated polymer molecular wire chemosensors for transition metal ion recognition and signaling, *Coord. Chem. Rev.* 253 (2009) 410–422.
- [4] J.-F. Peng, Y.-h. Song, P. Yuan, X.-y. Cui, G.-l. Qiu, The remediation of heavy metals contaminated sediment, *J. Hazard. Mater.* 161 (2-3) (2009) 633–640.
- [5] A. Mandal, M. Suresh, E. Suresh, S. Mishra, S. Mishra, A. Das, A chemosensor for heavy-transition metal ions in mixed aqueous-organic media, *Sens. Actuata. B: Chem.* 145 (2010) 32–38.
- [6] J. Zhao, D. Nelson, Fluorescence study of the interaction of Suwannee River fulvic acid with metal ions and Al³⁺-metal ion competition, *J. Inorg. Biochem.* 99 (2005) 383–396.
- [7] A. Mohd, A. Parwaz Khan, S. Bano, K. Siddiqi, Interaction of Clofazimine with divalent metal ions: a fluorescence quenching study, *J. Dispers. Sci. Technol.* 32 (2011) 1465–1469.
- [8] M. Montali, L. Prodi, N. Zaccheroni, Fluorescence quenching amplification in silica nanosensors for metal ions, *J. Mater. Chem.* 15 (2005) 2810.
- [9] Y. Chang, Y. Choi, A. Shin, Significant fluorescence quenching of anthrylaminobenzocrown ethers by paramagnetic metal cations, *Cheminform* 33 (2010).
- [10] T. Jennings, M. Singh, G. Strouse, Fluorescent lifetime quenching near d= 1.5 nm gold nanoparticles: probing NSET validity, *J. Am. Soc.* 128 (2006) 5462–5467.
- [11] N. Ruppich, W. Chiunan, R. Nutiu, S. Mei, K. Flora, Y. Li, et al., Quenching of fluorophore-labeled DNA oligonucleotides by divalent metal ions: implications for selection, design, and applications of signaling aptamers and signaling deoxyribozymes, *J. Am. Chem. Soc.* 128 (2006) 780–790.
- [12] Y. Posokhov, A. Kyrchenko, A. Ladokhin, Steady-state and time-resolved fluorescence quenching with transition metal ions as short-distance probes for protein conformation, *Anal. Biochem.* 407 (2010) 284–286.
- [13] Y. Xiao, A. Rowe, K. Plaxco, Electrochemical detection of parts-per-Billion lead via an electrode-bound DNAzyme assembly, *J. Am. Chem. Soc.* 129 (2007) 262–263.

- [14] M. Mohajeri, R. Mehdi Rezaee, A. Sahebkar, Cadmium-induced toxicity is rescued by curcumin: a review, *Biofactors* 43 (5) (2017) 645–661.
- [15] M. Irfan, S. Hayat, A. Ahmad, M. Alyemeni, Soil cadmium enrichment: allocation and plant physiological manifestations, *Saudi J. Biol. Sci.* 20 (2013) 1–10, <https://doi.org/10.1016/j.sjbs.2012.11.004>.
- [16] L. Patrick, Mercury toxicity and antioxidants: part 1: role of glutathione and alpha-lipoic acid in the treatment of mercury toxicity, *Altern. Med. Rev.* 7 (6) (2012) 456–471.
- [17] Z. Fang, J. Růžicka, E.H. Hansen, An efficient flow-injection system with on-line ion-exchange preconcentration for the determination of trace amounts of heavy metals by atomic absorption spectrometry, *Anal. Chim. Acta* 164 (1984) 23–39.
- [18] V.L. Dressler, D. Pozebon, A.J. Curtius, Determination of heavy metals by inductively coupled plasma mass spectrometry after on-line separation and preconcentration, *Spectrochim. Acta Part B: Atomic Spectrosc.* 53 (11) (1998) 1527–1539.
- [19] L. Cui, J. Wu, H. Ju, Electrochemical sensing of heavy metal ions with inorganic, organic and bio-materials, *Biosens. Bioelectron.* 63 (2015) 276–286.
- [20] S. Zeng, K.-T. Yong, I. Roy, X.-Q. Dinh, X. Yu, F. Luan, A review on functionalized gold nanoparticles for biosensing applications, *Plasmonics* 6 (3) (2011) 491–506.
- [21] C. Sreelakshmi, N. Goel, K. Datta, A. Addlagatta, R. Ummanni, B. Reddy, Green synthesis of curcumin capped gold nanoparticles and evaluation of their cytotoxicity, *Nanosci. Nanotechnol. Lett.* 5 (2013) 1258–1265, <https://doi.org/10.1166/nnl.2013.1678>.
- [22] L. Bechnak, K. Khalil, R. El Kurdi, R. Khnayer, D. Patra, Curcumin encapsulated colloidal amphiphilic block co-polymeric nanocapsules: colloidal nanocapsules enhance photodynamic and anticancer activities of curcumin, *Photochem. Photobiol. Sci.* 19 (2020) 1088–1098, <https://doi.org/10.1039/d0pp00032a>.
- [23] R. El Kurdi, D. Patra, Role of OH⁻ in the formation of highly selective gold nanowires at extreme pH: multi-fold enhancement in rate of catalytic reduction reaction by gold nanowires, *Phys. Chem. Chem. Phys.* 19 (2017) 5077–5090.
- [24] S. Al Shehab, R. El Kurdi, D. Patra, Curcumin mediated PEG thiol acid conjugated gold nanoparticles for the determination of melamine, *Microchem. J.* 153 (2020) 104382.
- [25] M. Desai, H. Basu, S. Saha, R. Singhal, S. Kailasa, One pot synthesis of fluorescent gold nanoclusters from Curcuma longa extract for independent detection of Cd²⁺, Zn²⁺ and Cu²⁺ ions with high sensitivity, *J. Mol. Liq.* 304 (2020) 112697, <https://doi.org/10.1016/j.molliq.2020.112697>.
- [26] M. Annadhasan, T. Muthukumarasamyvel, V.R. Sankar Babu, N. Rajendiran, Green synthesized silver and gold nanoparticles for colorimetric detection of Hg²⁺, Pb²⁺, and Mn²⁺ in aqueous medium, *ACS Sustain. Chem. Eng.* 2 (4) (2014) 887–896.
- [27] S. Manju, K. Sreenivasan, Functionalized nanoparticles for targeted drug delivery, *Biointegr. Med. Implant Mater.* (2010) 267–297.
- [28] K. Saha, S. Agasti, C. Kim, X. Li, V. Rotello, Gold nanoparticles in chemical and biological sensing, *Chem. Rev.* 112 (2012) 2739–2779.
- [29] B. Paul, A. Tiwari, A brief review on the application of gold nanoparticles as sensors in multi dimensional aspects IOSR, *J. Environ. Sci. Toxicol. Food Technol. (IOSR-JESTFT)* 1 (4) (2020) 01–07, e-ISSN: 2319-2402, p-ISSN: 2319-2399, www.iosrjournals.org.
- [30] A. Sugunan, C. Thanachayanont, J. Dutta, J.G. Hilborn, Heavy-metal ion sensors using chitosan-capped gold nanoparticles, *Sci. Technol. Adv. Mater.* 6 (3-4) (2005) 335–340.
- [31] Z. Osner, R. Holz, D. Becker, An analytical method for detecting toxic metal cations using cyclotrimerethylene derivative capped gold nanoparticles, *Tetrahedron Lett.* 56 (40) (2015) 5419–5423.
- [32] J. Jockerst, T. Lobovkina, R. Zare, S. Gambhir, Nanoparticle PEGylation for imaging and therapy, *Nanomedicine.* 6 (2011) 715–728, <https://doi.org/10.2217/nm.11.19>.
- [33] S. Smitha, D. Philip, K. Gopchandran, Green synthesis of gold nanoparticles using Cinnamomum zeylanicum leaf broth, *Spectrochim. Acta Part A: Molecul. Biomolecul. Spectrosc.* 74 (2009) 735–739.
- [34] K. Sneha, M. Sathishkumar, S. Kim, Y. Yun, Counter ions and temperature incorporated tailoring of biogenic gold nanoparticles, *Process Biochem.* 45 (2010) 1450–1458.
- [35] X. Chen, L. Zou, J. Niu, W. Liu, S. Peng, C. Liu, The Stability, Sustained release and cellular antioxidant activity of curcumin nanoliposomes, *Molecules* 20 (8) (2015) 14293–14311.
- [36] B. Korthals, M. Morant-Miñana, M. Schmid, S. Mecking, Functionalization of polymer nanoparticles by Thiol–Ene addition, *Macromolecules* 43 (19) (2010) 8071–8078.
- [37] J. Manson, D. Kumar, B. Meenan, D. Dixon, Polyethylene glycol functionalized gold nanoparticles: the influence of capping density on stability in various media, *Gold Bull.* 44 (2011) 99–105.
- [38] D. Patra, C. Barakat, Synchronous fluorescence spectroscopic study of solvatochromic curcumin dye, *Spectrochim. Acta Part A: Molecul. Biomolecul. Spectrosc* 79 (2011) 1034–1041.
- [39] S. Prabu, S. Mohamad, Curcumin/beta-cyclodextrin inclusion complex as a new “turn-off” fluorescent sensor system for sensitive recognition of mercury ion, *J. Molecul. Struct.* 1204 (2020), 127528.
- [40] S.-H. Kim, S.-Y. Gwon, S.M. Burkinshaw, Y.-A. Son, The photo- and electrophysical properties of curcumin in aqueous solution, *Spectrochim. Acta Part A* 76 (2010) 384–387.
- [41] M. Swierczewska, S. Lee, X. Chen, The design and application of fluorophore-gold nanoparticle activatable probes, *Phys. Chem. Chem. Phys.* 13 (2011) 9929.
- [42] J. Albani, Chapter 2: fluorescence quenching. *Structure and Dynamics Of Macromolecules: Absorption And Fluorescence Studies*, 2004, pp. 141–192, <https://doi.org/10.1016/b978-044451449-3/50004-6>.

- [43] H. Crouse, J. Potoma, F. Nejrabi, D. Snyder, B. Chohan, S. Basu, Quenching of tryptophan fluorescence in various proteins by a series of small nickel complexes, *Dalton Trans.* 41 (2012) 2720.
- [44] D. Patra, A.K. Mishra, Determination of quenching inhibition factor and selective fluorescence quenching study of perylene, pyrene and fluoranthene in micelle by cetyl pyridinium chloride as a hydrophobic quencher molecule, *Polycyc. Aromat. Comp.* 18 (4) (2001) 367–380.
- [45] D. Patra, C. Barakat, Time-resolved fluorescence study during denaturation and renaturation of curcumin-myoglobin complex, *Int. J. Biol. Macromol.* 50 (2012) 885–890.